



Theoretical study of three predominant tautomers of 2-oxo-6-methylpurine and their two transition state structures

Jong Hwa Kim *

Department of Chemistry, Alabama A&M University, Normal, AL 35762, USA

ARTICLE INFO

Article history:

Received 21 September 2009

Revised 24 October 2009

Accepted 9 November 2009

Available online 13 November 2009

Keywords:

2-Oxo-6-methylpurine

2-Hydroxy-6-methylpurine

Tautomerism

Xanthine oxidase

Intramolecular proton transfer

ABSTRACT

The three predominantly stable tautomers of 2-oxo-6-methylpurine were studied in gas phase and aqueous solution by means of quantum mechanical calculations. Two transition state structures connecting these three tautomeric forms on the free energy surface were determined. The activation free energy for the intramolecular proton transfer in gas phase was calculated to be considerably smaller than the bond energy of either N–H or O–H: 59.01 and 30.37 kcal/mol for N9→N3 and N1→O2, respectively, obtained at the QCISD(T)/6-31G+(d)//MP2(full)/6-31G(d) level of theory.

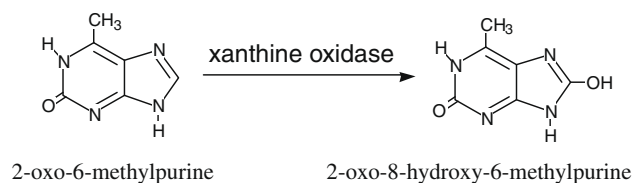
© 2009 Elsevier Ltd. All rights reserved.

For a few decades, extensive kinetic and spectroscopic studies have been performed regarding the enzyme–substrate reaction taking place in the course of the reductive half-reaction at the molybdenum center of xanthine oxidase, the prototypical mononuclear molybdenum enzyme.¹ Recently, computational methods have begun to be employed in studying the geometry of the molybdenum center of xanthine oxidase and to understand the possible reaction mechanism for oxidation of the substrate.^{2–5} Although a vast amount of information on this molybdenum is available,^{6,7} including determination of the crystal structures of the enzyme and the enzyme–substrate complex,⁸ the detailed reaction mechanism of molybdenum reduction/oxidation during catalysis is still to be determined. 2-Oxo-6-methylpurine (also called 2-hydroxy-6-methylpurine) has been a very useful substrate in the mechanistic studies of the reductive half-reaction of xanthine oxidase,⁹ since oxidation of 2-oxo-6-methylpurine to 2-oxo-8-hydroxy-6-methylpurine (Scheme 1) at the molybdenum center is so slow that the kinetics of this substrate oxidation can be studied with ease and accuracy. A number of mechanistic studies of xanthine oxidase have focused on the characterization of the reaction intermediate responsible for the so-called ‘very rapid’ Mo(V) EPR signal, which is believed to be the species where 2-oxo-8-hydroxy-6-methylpurine is bound to the enzyme molybdenum via the Mo–O–C8 bond.^{4,10}

Recent quantum mechanical studies of a few substrates of xanthine oxidase¹¹ revealed that three out of nine tautomeric forms of

2-oxo-6-methylpurine are predominantly stable, while only one preferred tautomeric form exists for each of the other substrates, xanthine and lumazine. In this Letter, the three predominant tautomeric forms of 2-oxo-6-methylpurine and energetics of interconversion among these three tautomers in the absence of solvent molecules are investigated by using high-level quantum mechanical methods.

Figure 1a shows the three predominant tautomers of 2-oxo-6-methylpurine, named omp13, omp19, and omp29, with ‘omp’ as an abbreviation of 2-oxo-6-methylpurine. Table 1 shows the relative stability of these three tautomers, based on the calculations using high-level ab initio quantum mechanical calculations (MP2, MP4, and QCISD) and DFT calculations (B3LYP) with larger basis sets. The data suggest that the enol form (omp29), rather than the keto forms (omp13 and omp19), is the most stable tautomeric form in gas phase. (When the single-point energies were calculated using the MP4(SDTQ)/6-31+G(d) method, the total energy of omp13 was lower than that of omp29 by 0.04 kcal/mol, implying



Scheme 1. Conversion of 2-oxo-6-methylpurine to 2-oxo-8-hydroxy-6-methylpurine by xanthine oxidase.

* Tel.: +1 256 372 4935; fax: +1 256 372 8288.

E-mail address: jong.kim@aamu.edu

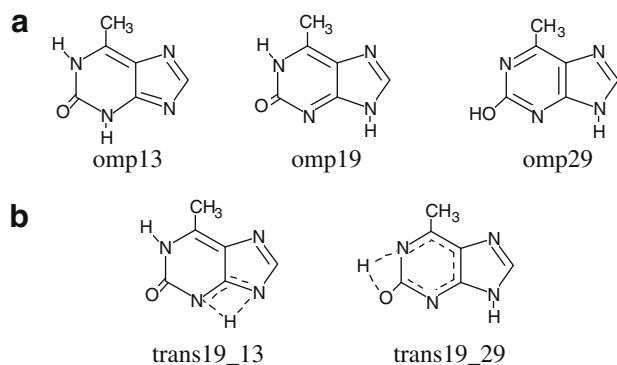


Figure 1. (a) The three most stable tautomers of 2-oxo-6-methylpurine and (b) the two transition structures in the path of the intramolecular proton migration in gas phase.

Table 1

The relative energy differences (in kcal/mol) at 0 K and 1 atm in gas phase for the three 2-oxo-6-methylpurine tautomers with the most stable form set to 0

Methods	omp13	omp19	omp13
QCISD(T)/6-31G+(d)//MP2(full)/6-31G(d)	0.66	2.35	0.00
MP4(SDTQ)/6-31+G(d)//MP2(full)/6-31G(d)	0.00	1.90	0.04
MP2(full)/6-311+G(3df,2pd)//MP2(full)/6-31G(d)	3.80	4.84	0.00
B3LYP/6-311++G(3df,3pd)//B3LYP/6-311+G(2d,p)	0.99	0.98	0.00

that the energy of omp13 is virtually the same as that of omp29.) These findings agree with the previous study performed using DFT calculations with smaller basis sets.¹¹ Since the relative energy differences among these three tautomers are very small, it is very likely that 2-oxo-6-methylpurine exists mostly in a mixture of these three tautomeric forms in gas phase.

Whereas xanthine binds xanthine oxidase with its C6 carbonyl positioned to interact with the arginine-880 residue in stabilizing the Mo(V) transition, a recent study of the crystal structure shows that 2-oxo-6-methylpurine orients in the active site of the enzyme, with its C2 carbonyl group interacting with the arginine-880 residue.⁸ Since omp29 with its hydroxy group at C2 is unlikely to interact with the aforementioned arginine residues, either omp13 or omp19 should be a favored tautomeric form of 2-oxo-6-methylpurine at the active site of the enzyme. The calculations in this study show that omp19 becomes noticeably more stable than the other two tautomeric forms (by more than 3 kcal/mol) in aqueous solution. This probably is because the decrease in Gibbs free energy when omp19 is transferred from gas phase to water is noticeably larger than when either of the other two tautomeric forms is transferred to aqueous solution; the solvation free energy has been calculated to be -24.96 , -21.78 , and -20.19 kcal/mol for omp19, omp13, and omp29, respectively, as seen in Table 2.

While omp19 is the most convincingly stable in aqueous solution among all the possible tautomeric forms of 2-oxo-6-methylpurine, the stability advantage of omp29 over omp13 and omp19 in

Table 2

Relative energy (ΔE_g) and free energy (ΔG_g) at 298 K in gas phase, and solvation free energy (ΔG_s), for the three most stable tautomers of 2-oxo-6-methylpurine

Tautomers	ΔE_g (kcal/mol)	ΔG_g (kcal/mol)	ΔG_s (kcal/mol)
omp29	0.00	0.00	-20.19
omp19	1.06	1.04	-24.96
omp13	1.13	1.13	-21.78

All calculations were carried out at B3LYP/6-311+G(2d,p) level of theory. Thermal energy has been scaled by 0.989.

gas phase is very small. As stated previously, it is probable that 2-oxo-6-methylpurine exists in a mixture of these three tautomeric forms in gas phase. Studies of intramolecular proton transfer and tautomerism in gaseous glycine by computational methods have been reported.^{12,13} It is therefore of interest to study the energetics of interconversion of the tautomers of 2-oxy-6-methylpurine into one another via intramolecular proton transfer.

The two first-order saddle points on the free energy surface of these three tautomers were located using the STQN method¹⁴ at the MP2(full)/6-31G(d) level of theory. These first-order saddle points have been confirmed, by IRC calculations, to be the two transition structures encountered in the course of interconversion among the three tautomers, and are thus named trans19_13 (between omp19 and omp13) and trans19_29 (between omp19 and omp29). These are shown in Figure 1b. The calculations show that the energy barrier between omp19 and omp29 is about 30 kcal/mol, while the energy barrier between omp13 and omp19 is about 60 kcal/mol on the free energy surface diagram, as can be seen in Table 3 and Figure 2. These values are considerably smaller than the bond energy of either N–H or O–H. The fact that the energy barrier between omp13 and omp19 is about twice that between omp29 and omp19 can be understood in terms of the Mulliken charge data. For the omp13 to omp19 conversion, the transfer of proton has to take place from very negative N3 (-0.951) to much less negative N9 (-0.611). On the other hand, for the omp29 to omp19 conversion, the transfer of proton needs to take place from O2 (-0.726) to almost equally negative N1 (-0.698) in omp29. In addition, the proton needs to travel a longer distance in the omp13 to omp19 conversion than in the omp29 to omp19 conversion.

Starting from omp19, the larger energy barrier for the N9→N3 proton migration (59 kcal/mol), compared to that for the N1→O2 proton migration (30 kcal/mol), is also implicated in the lengths and angles of transient bonds in the transition state structures (Table 4). While the transient N3–H and N9–H bonds in trans19_13 are about 0.45 Å longer than regular N–H bonds, the N1–H in trans19_29 is only about 0.3 Å longer than regular N–H bonds. In trans19_29, the C2–O2 bond length of 1.29 Å is between typical C=O (1.22 Å) and C–O (1.43 Å) bonds, demonstrating the transition from C=O to C–O.

In conclusion, omp19 is the most stable in aqueous solution among all the possible tautomeric forms of 2-oxo-6-methylpurine. In gas phase, however, the difference in stability among these three tautomers is very small. Starting from omp19, the activation free energy for the N9→N3 proton migration is twice as large as that for the N1→O2 proton migration.

All the calculations were carried out with GAUSSIAN 98¹⁵ or GAUSSIAN 03¹⁶ set of programs on the Cray SV1, Cray XD1, and SGI Altix housed at the Alabama Supercomputer Center in Huntsville, AL. Geometries of the tautomers and the transition structures were first optimized by the MP2 method¹⁷ with the 6-31G(d) basis set (MP2(full)/6-31G(d)), and a hybrid Hartree–Fock/density functional theory (HF/DFT) method, employing Becke's three-parameter exchange functional¹⁸ and Lee, Yang, and Parr's correlation functional (B3LYP) in

Table 3

Relative free energy (ΔG_g) at 298 K in gas phase for the three most stable tautomers of 2-oxo-6-methylpurine and their transition state structures

Tautomers	ΔG_g (kcal/mol)
omp29	0.00
trans19_29	33.86
omp19	3.49
trans19_13	62.50
omp13	1.91

All calculations were carried out at the MP2(full)/6-31G(d) level of theory. Thermal energy has been scaled by 0.9646.

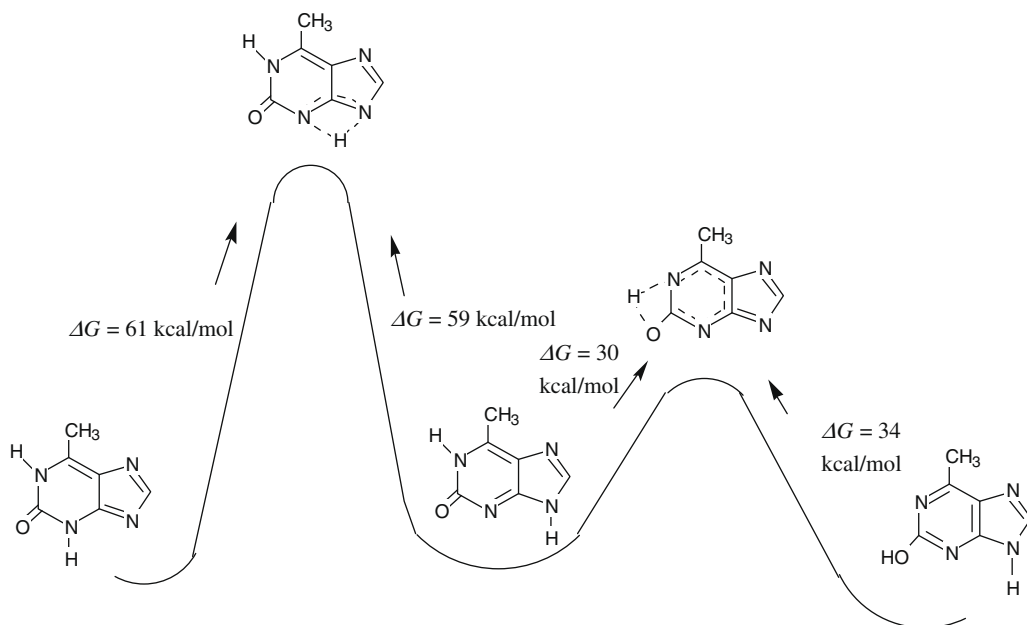


Figure 2. The potential energy surface diagram of the three tautomers in gas phase determined with the QCISD(T)/6-31G+(d)//MP2(full)/6-31G(d) method.

Table 4

Lengths and angles involving transient bonds in the transition state structures obtained at the MP2(full)/6-31G(d) level of theory

trans19_29		trans19_13	
N1...H	1.281 Å	N3...H	1.441 Å
C2...O2	1.290 Å		
O2...H	1.384 Å	N9...H	1.426 Å
N1...H...O2	105.5°	N3...H...N9	100.6°
N1-C2-O2	104.4°	N3-C4-N9	112.8°

a parametrized fashion,¹⁹ with the 6-311+G(2d,p) basis set (B3LYP/6-311+G(2d,p)). Optimizations were done using the Bery algorithm,²⁰ with the initial Hessian estimated by using force constants from a valence force field. The transition structures were searched by means of the synchronous transit-guided quasi-Newton (STQN) method¹⁴ using the quadratic synchronous transition (QST2) option with MP2(full)/6-31G(d). The transition structures were confirmed using intrinsic reaction coordinate (IRC) calculations²¹ with MP2(full)/6-31G(d). Single-point energy calculations for the tautomers and for the transition structures were performed using the QCISD(T)²² method (QCISD(T)/6-31G+(d)), the full MP4 method (MP4(SDTQ)/6-31+G(d)), the MP2 method with a larger basis set (MP2(full)/6-311+G(3df,2pd)), and the B3LYP/6-311+G(3df,3pd) levels of theory. The solvent effects on the energetics of these stable tautomers were evaluated by means of the Conductor Polarized Continuum Model (CPCM).²³ All CPCM calculations were carried out with a dielectric constant (ϵ) of 78.39, approximating bulk water.

Acknowledgment

This work was made possible in part by a grant of high performance computing resources and technical support from the Alabama Supercomputer Center.

References and notes

- Hille, R. *Chem. Rev.* **1996**, *96*, 2757–2816.
- Voityuk, A. V.; Albert, A.; Köstlmeier, S.; Nasluuzov, V. A.; Neyman, K. M.; Hof, P.; Huber, R.; Romão, M. J.; Rösch, N. *J. Am. Chem. Soc.* **1997**, *119*, 3159–3160.
- Ilich, P.; Hille, R. *J. Am. Chem. Soc.* **2002**, *124*, 6796–6797.
- Bayse, C. A. *Inorg. Chem.* **2006**, *45*, 2199–2202.
- Amano, T.; Ochi, N.; Sato, H.; Sakaki, S. *J. Am. Chem. Soc.* **2007**, *129*, 8131–8138.
- Enroth, C.; Eger, B. T.; Okamoto, K.; Nishino, T.; Pai, E. F. *Proc. Natl. Acad. Sci. U.S.A.* **2000**, *97*, 10723–10728.
- Okamoto, K.; Matsumoto, K.; Hille, R.; Eger, B. T.; Pai, E. F.; Nishino, T. *Proc. Natl. Acad. Sci. U.S.A.* **2004**, *101*, 7931–7936.
- Pauff, A. M.; Zhang, J.; Bell, C. E.; Hille, R. *J. Biol. Chem.* **2008**, *283*, 4818–4824.
- Kim, J. H.; Ryan, M. G.; Knaut, H.; Hille, R. *J. Biol. Chem.* **1996**, *271*, 6771–6780.
- Choi, E. Y.; Stockert, A. L.; Leimkuhler, S.; Hille, R. *J. Inorg. Biochem.* **2004**, *98*, 841–848.
- Kim, J. H.; Odutola, J. A.; Popham, J.; Jones, L.; von Laven, S. *J. Inorg. Biochem.* **2001**, *84*, 145–150.
- Zhang, K.; Chung-Phillips, A. *J. Chem. Inf. Comput. Sci.* **1999**, *39*, 382–395.
- Rodriguez, C. F.; Cunje, A.; Shoeib, T.; Chu, I. K.; Hopkins, A. C.; Siu, K. W. M. *J. Am. Chem. Soc.* **2001**, *123*, 3006–3012.
- Peng, C.; Schlegel, H. B. *Israel J. Chem.* **1994**, *33*, 449–454.
- Frisch, M. J.; Trucks, G. W.; Schlegel, H. B.; Scuseria, G. E.; Robb, M. A.; Cheeseman, J. R.; Zakrzewski, V. G.; Montgomery, J. A., Jr.; Stratmann, R. E.; Burant, J. C.; Dapprich, S.; Millam, J. M.; Daniels, A. D.; Kudin, K. N.; Strain, M. C.; Farkas, O.; Tomasi, J.; Barone, V.; Cossi, M.; Cammi, R.; Mennucci, B.; Pomelli, C.; Adamo, C.; Clifford, S.; Ochterski, J.; Petersson, G. A.; Ayala, P. Y.; Cui, Q.; Morokuma, K.; Malick, D. K.; Rabuck, A. D.; Raghavachari, K.; Foresman, J. B.; Cioslowski, J.; Ortiz, J. V.; Baboul, A. G.; Stefanov, B. B.; Liu, G.; Liashenko, A.; Piskorz, P.; Komaromi, I.; Gomperts, R.; Martin, R. L.; Fox, D. J.; Keith, T.; Al-Laham, M. A.; Peng, C. Y.; Nanayakkara, A.; Gonzalez, C.; Challacombe, M.; Gill, P. M. W.; Johnson, B.; Chen, W.; Wong, M. W.; Andres, J. L.; Austin, A. J.; Cammi, R.; Pomelli, C.; Ochterski, J. W.; Ayala, P. Y.; Morokuma, K.; Voth, G. A.; Salvador, P.; Dannenberg, J. J.; Zakrzewski, V. G.; Dapprich, S.; Daniels, A. D.; Strain, M. C.; Farkas, O.; Malick, D. K.; Rabuck, A. D.; Raghavachari, K.; Foresman, J. B.; Ortiz, J. V.; Baboul, A. G.; Clifford, S.; Cioslowski, J.; Stefanov, B. B.; Liu, G.; Liashenko, A.; Piskorz, P.; Komaromi, I.; Martin, R. L.; Fox, D. J.; Keith, T.; Al-Laham, M. A.; Peng, C. Y.; Nanayakkara, A.; Challacombe, M.; Gill, P. M. W.; Johnson, B.; Chen, W.; Wong, M. W.; Gonzalez, C.; Pople, J. A.; *GAUSSIAN 03, Revision C.02*, Gaussian: Wallingford, CT, 2004.
- Head-Gordon, M.; Pople, J. A.; Frisch, M. J. *J. Chem. Phys. Lett.* **1988**, *153*, 503–506.
- Becke, A. D. *J. Chem. Phys.* **1993**, *98*, 5648–5652.
- Lee, C.; Yang, W.; Parr, R. G. *Phys. Rev.* **1988**, *37B*, 785–789.
- Schlegel, H. B. *J. Comput. Chem.* **1982**, *3*, 214–218.
- Gonzalez, C.; Schlegel, H. B. *J. Chem. Phys.* **1989**, *90*, 2154–2161.
- Pople, J. A.; Head-Gordon, M.; Raghavachari, K. *J. Chem. Phys.* **1987**, *87*, 5968–5975.
- Barone, V.; Cossi, M. *J. Phys. Chem. A* **1998**, *102*, 1995–2001.